Applied Surface Science Advances 6 (2021) 100169

Contents lists available at ScienceDirect

Applied Surface Science Advances

journal homepage: www.sciencedirect.com/journal/applied-surface-science-advances

Dry etching of monocrystalline silicon using a laser-induced reactive micro plasma

Robert Heinke [a], Martin Ehrhardt [a,*], Pierre Lorenz [a], Klaus Zimmer [a,*]

[a] Leibniz Institute of Surface Engineering (IOM), Permoserstr. 15, 04318 Leipzig, Germany

ARTICLE INFO

Keywords:
Plasma formation
Laser
Reactive etching
Si
CF_4

ABSTRACT

Dry etching is a prevalent technique for pattern transfer and material removal in microelectronics, optics and photonics due to its high precision material removal with low surface and subsurface damage. These processes, including reactive ion etching (RIE) and plasma etching (PE), are performed at vacuum conditions and provide high selectivity and vertical side wall etched patterns but create high costs and efforts in maintenance due to the required machinery.

In contrast to electrically generated plasmas, laser-induced micro plasmas are controllable sources of reactive species in gases at atmospheric pressure that can be used for dry etching of materials.

In the present study, we have demonstrated the laser-induced plasma etching of monocrystalline silicon. A Ti:Sapphire laser has been used for igniting an optically pumped plasma in a CF_4/O_2 gas mixture near atmospheric pressure. The influence of process parameters, like substrate temperature, O_2 concentration, plasma-surface distance, etching duration, pulse energy and crystal orientation on etching rate and surface morphology has been investigated.

Typical etching rates of 2–12 µm x min^{-1} can be achieved by varying mentioned parameters with a decreasing etching rate during the process. Different morphologies can be observed due to the parameters set, smooth as well as rough surfaces or even inverted pyramids.

The presented etching method provides an approach for precise machining of silicon surfaces with good surface qualities near atmospheric pressure and sufficiently high material removal rates for ultraprecise surface machining.

1. Introduction

Ultraprecise machining (UPM) with pulsed laser radiation for applications in optics, electronics and microfluidics is still a challenge as the commonly used laser ablation process does not fulfil important requirements for UPM such as low defect density, low material removal rate and smooth surface processing. The surface roughness and subsurface damage are too high for various of microscale applications and the typical material removal rate of 10–100 nm per laser pulse are too high for manufacturing with high vertical accuracy [1]. However, the direct writing capabilities, processing at normal conditions (no vacuum required) as well as the precise control of the laser beam tool, favour the utilization of lasers for surface processing.

The most common techniques used in microelectronics for material removal and pattern transfer are etching processes, that are divided into wet and dry methods according to the different reactive media used.

Plasma etching is a widely used dry etching method, which is normally performed at low pressure. The plasma can be generated in different ways, most commonly powered by rf-electrodes or microwaves. Large concentrations of reactive species without an extensive heating of the sample can be achieved in this way.

Reactive ion etching (RIE) is an advanced dry etching technique, which uses an electric field to accelerate ions in the plasma to the substrate that stimulate chemical processes at the surface, resulting in additional physically stimulated removal and offer the possibility of anisotropic etching. Traditional dry etching techniques such as processes as RIE or PE are wafer level etching techniques and are utilized for pattern transfer of lithographically produced masks into thin films and surfaces with high lateral resolution. Related to the ion bombardment of the surface is the possibility of producing defects and the implanting of impurities into the subsurface [2–4]. The complexity and costs in procurement and operation are a big disadvantage for these low-pressure

* Corresponding authors.
E-mail addresses: martin.ehrhardt@iom-leipzig.de (M. Ehrhardt), klaus.zimmer@iom-leipzig.de (K. Zimmer).

https://doi.org/10.1016/j.apsadv.2021.100169
Received 3 June 2021; Received in revised form 31 August 2021; Accepted 14 September 2021
Available online 23 September 2021

processes.

Direct writing processes with plasmas realizing a localized etching are rather rare and can be applied for ultraprecise surface machining that is needed for high fidelity optics [5,6].

Atmospheric pressure plasma jets (APPJ) allow an almost purely chemical dry etching of different materials at atmospheric pressures. The sustaining of the plasma discharge under these conditions requires the adjustment of the excitation process, for example by higher voltages [7,8]. APPJ is subject of numerous investigations for etching or surface figuring [5], amongst other materials for the machining of silicon [9–11].

However, not only the substrate is exposed to the plasma species and ions but the electrodes, nozzles and other parts of the equipment, too. This can result in contaminations of the plasma and deteriorations of the etching quality.

Direct writing by laser ablation is regularly used for surface machining of various materials. However, laser ablation is not well suited for UPM due to the typical ablation rates and the generated roughness. Laser-induced backside wet etching (LIBWE) is an approach to enhance the precision and surface quality of laser processing. A laser beam penetrates a transparent substrate and gets absorbed by a liquid covering the substrate backside. The normally aqueous or hydrocarbon solution of dyes and solvents heats up and etches the rear surface. The laser wavelength must ensure the transparency of the substrate and the high absorption in the dye. This approach has advantages for etching glass materials [1,12,13].

The challenge of high-quality direct laser writing is approached by utilizing a laser plasma ignited in the focal range and stimulating a plasma material removal process that combines the easy handling of the laser process with the high surface quality of plasma etching. Thereby the plasma is ignited by optical breakdown with an ultra-short pulsed laser at atmospheric pressures.

The application of laser-induced plasmas in air for glass processing was already studied [14]. Due to the near surface focussing, surface contaminations and signs of melting and evaporation were found [15]. The application of laser-induced reactive plasmas for etching SiO_2 has been investigated recently [16]. Traditionally, laser-induced plasmas (LIP) are mostly used for analytical purposes, especially for laser-induced breakdown spectroscopy (LIBS) [17,18].

In the present study dry etching of silicon using a laser-induced plasma, ignited in a CF_4/O_2 gas mixture at normal pressure is investigated. In relation to former studies on dry and wet etching of silicon, the etching process as well as the achievable surface quality needs to be studied.

2. Material and methods

A sketch of the experimental setup is shown in Figs. 1 and 2. The process chamber that includes the sample etc. is attached to a computer-controlled x-y-z stage system, allowing the movement of the whole setup relative to the LIP (laser-induced plasma). The chamber encloses the sample holder that is attached to a silicon nitride resistance heater with that the clamped samples can be heated up to 500 °C. The sample temperature (T_S) is varied in the range of 120–400 °C.

An ultrashort pulse laser system with a wavelength (λ) of 775 nm, a pulse length (t_p) of 150 fs, and a pulse repetition rate (f_P) of 1000 Hz provides the laser beam. The laser pulse energy (E_P), that was varied by a computer-controlled attenuator, was selected in a range from 550 to 1070 μJ. A 60 mm focal length lens focuses the beam through an entrance window into the chamber, igniting a plasma in the focal point by optical breakdown in the etching gas.

To avoid direct interaction of laser and silicon, the beam propagates parallel to the sample surface. The distance of the laser spot to the samples surface, called plasma-surface distance (d_{PS}), has been varied by the stages from 100 to 220 μm. Two cameras installed orthogonal to each other outside the chamber are enabled to image the plasma and the substrate via additional windows attached to the chamber walls to determine the relative position of the plasma to the substrate.

The etching gas mixture is composed of tetrafluoromethane (CF_4) and oxygen (O_2). The process gases are fed into the chamber by a hose connected to a CF_4 and a O_2 flow controller. The total flow of 720 sccm was held constant at the experiments resulting in a complete gas

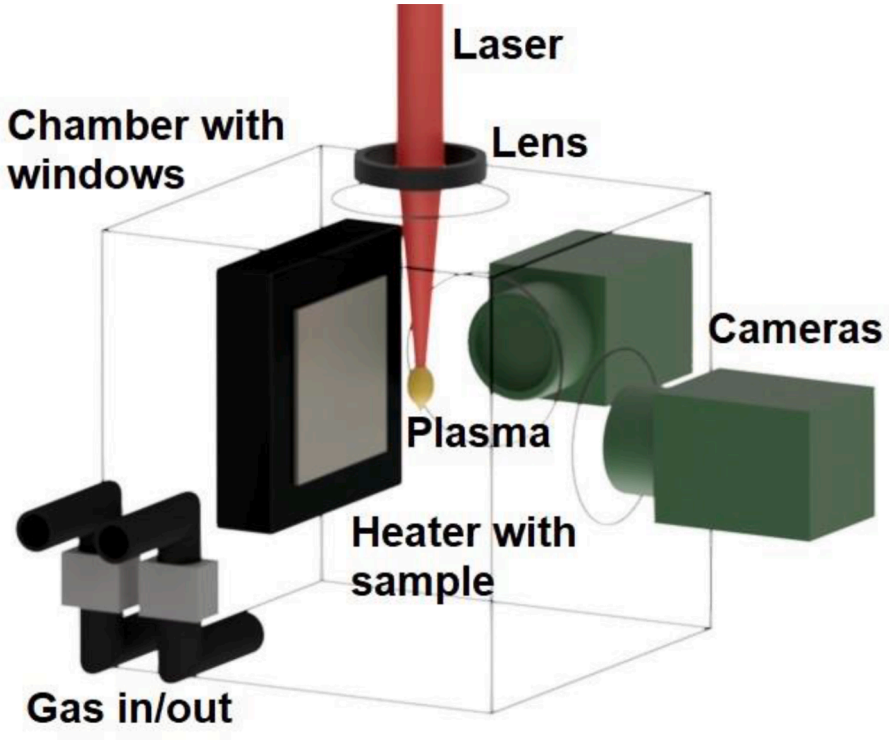

Fig. 1. Sketch of the experimental setup.

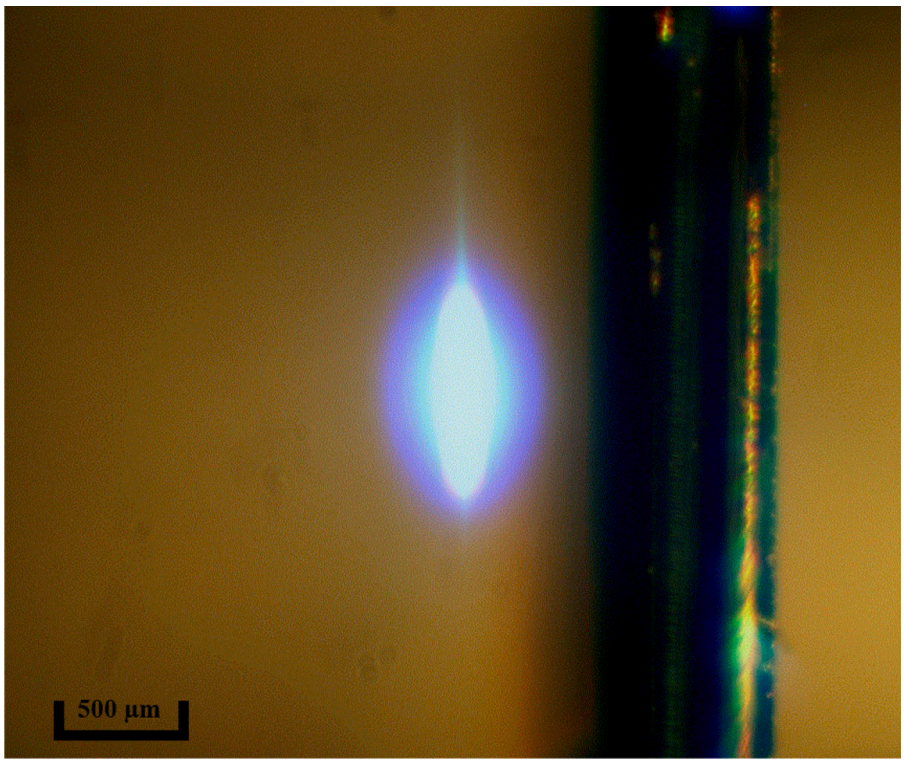

Fig. 2. Image of a laser-induced plasma next to the silicon substrate. The beam of an ultrashort puled laser is focussed near the silicon substrate inducing a plasma by optical breakdown in a CF_4/O_2 gas mixture.

exchange in the chamber every 30 s. The amount of oxygen was varied in the limits of 0–50 vol.-%. The etching gas was exhausted by a vacuum pump that can be throttled to control the pressure inside the chamber; for these experiments a pressure of 800±50 mbar (pressure gauge) was used.

Silicon substrates were cut into 10 × 10 mm squares out of a one side polished ⟨100⟩ silicon wafer (Si <100>).

<110> and <111>-oriented silicon has been studied too for comparison. In order to remove impurities from the surface, all samples have been subject to RCA cleaning [19]. They were subsequently dried by spin-off and heating for 3 min at 115 °C. After a maximal storage time of 3 days in a dry atmosphere, the samples were used for the experiments.

The etching footprints in the silicon, originated by material removal and hereinafter referred to as etching grooves, are analysed after etching by white light interferometry (WLIM, NPFLEX, Bruker) to obtain the etching grooves profile and maximal etching depths. The maximal etch groove depth was used to calculate the average (related to time) etching rate by dividing the etching depth by the etching time. To achieve a better comparability to other dry etching methods, this time-based system was chosen. Since the material removal rate for laser processes is related to the number of pulses, it should be mentioned, that the time-based removal rate can be converted by dividing by 60,000 (pulses per minute).

The surface after etching is imaged by SEM (Gemini Ultra 55, Zeiss) and AFM (Dimension ICON, Bruker) to investigate the influence of the etching parameters on roughness and morphology of the etched surface. AFM measurements are carried out in tapping mode™ and a xy-closed loop configuration across a scanning area of 10 µm x 10 µm.

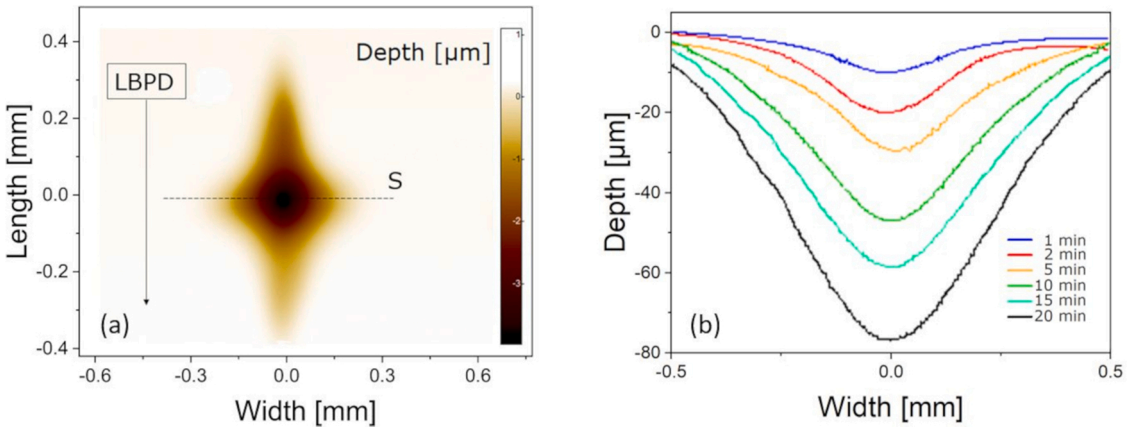

Fig. 3. WLIM imaged etching grooves. a) Contour plot of a typical etching groove with S as an example for a cross section. b) Cross section profiles of the etching grooves with different depths due to different etching times Parameter: (a) $t_E = 1$ min; $E_P = 700$ µJ, $T_S = 230$ °C, p_{tot}= 800 mbar, O_2= 17 vol.-%. (b) $E_P = 880$ µJ, $T_S = 330$ °C, $d_{PS} = 140$ µm, $p_{tot} = 800$ mbar, $O_2 = 17$ vol.-%.

3. Results

A typical etching groove is shown in Fig. 3a. The shape of the silicon etching using the reactive micro plasma resembles a kind of rhomboid pattern. The line shown in addition marks the position of the cross sections shown in Fig. 3b and representing etching grooves with different etching times. The long axis is given by the laser beam propagation direction (LBPD). Due to the rather long focal length the laser spot is rather long (l_{Re}=18 μm) compared to the spot size with 2.1 μm [18].

While the groove gets deeper with increasing process time, the lateral size (length and width of the rhomboid) increases significantly less, resulting in steeper groove walls. Length and width increase similarly fast, but the starting value of the length is higher. Therefore, the shape for low depths is more elongated in laser beam propagation compared to deeper etching grooves.

The temperature dependence of the etching rate is shown in Fig. 4. The sample temperature (T_S) is varied while all other etching process parameters such as etching time (t_E) of 3 min with 920 μJ pulse energy (E_P) and an O_2 content of 17 vol.-% are fixed. The plasma is generated in 140 μm distance to the surface (d_{PS}). The etching rate of <100> Si rises linearly with increasing substrate temperature. This linear temperature dependence is somehow surprising as for thermally activated chemical processes an exponential dependence can be expected.

With the same parameters but a fixed sample temperature of 230 °C, the influence of the plasma-surface distance is investigated in a range of 100 to 220 μm. The silicon etching rate decreases continuously with enlarged distances between the LIP and the Si surface as shown in Fig. 5; the extrapolation of the linear fitted experimental data suggests an etching threshold at a distance of 230 μm.

The influence of the oxygen content of the etching gas on the etching rate can be seen in Fig. 6. With increasing oxygen content, first the etching rate is almost constant but decreases after the oxygen content exceeds 15%. Across the whole range of 0–50 vol.-% the etching rate can be fitted by a parabolic function, but a linear relation can be suggested for the second range also. Images from the LIP taken with the cameras do not show any differences for plasmas ignited at different oxygen concentrations in size, color or brightness.

To determine the stability of the etching process the etching depth was measured and the surface topography studied with increasing etching time. The results, depicted in Fig. 7, show a continuous decrease of the average etching rate until a value of approximately 4 μm x min^{-1} at which saturation of the rate happens. The averaged etching rate can be fitted by $f_1(t) = a\text{-}b*c^t$ with a saturation limit for $t\rightarrow\infty$ of 3.8 μm x min^{-1}, as shown in Fig. 7 too. However, the slope of the etching depth over time is almost linear and suggest a rather constant etching rate except the very first time. Therefore, in addition two straight lines are sketched that are fitted to the etching depth and result in etching rates of 10.8 and 3.3 μm x min^{-1}, respectively.

Taking the repetition rate of 1 kHz into account an etching depth of 0.063 nm for a laser pulse can be calculated, which is fair below the lattice constant of silicon (0.54 nm) [20], so that an etching precision of less than an atomic layer can be achieved.

The etching rate increases linearly with an increasing laser pulse energy, as shown in Fig. 8. The visible glow of the plasma increases in dimensions as well as in brightness with a higher pulse energy, as shown in [16]. The minimal pulse energy to ignite a visible plasma in the gas mixture is 40 μJ, but for less than 500 μJ pulse energy no evidence of etching can be seen at 140 μm plasma distance. A similar etching threshold at 460 μJ can be extracted by extrapolating the linear fit shown in Fig. 8.

Further, different oriented crystalline samples have been etched with the same condition. The etching rates for different crystal orientations that are etched with identical parameters for 2, 5 and 10 min (p_{tot} = 800 mbar; E_p = 920 μJ; d_{PS} = 140 μm; O_2 = 17 vol.-%; T_S = 230 °C) can be seen in Fig. 9.

The influence of the crystal orientation on the etching rate is of great significance for crystallographic etching. Crystallographic etching is typically observed in wet etching processes with alkaline etchants [21]. Contrary to wet etching, the etching rates of silicon with <111> orientation is the highest, while <100> and <110> orientations having approximately the same etching rates.

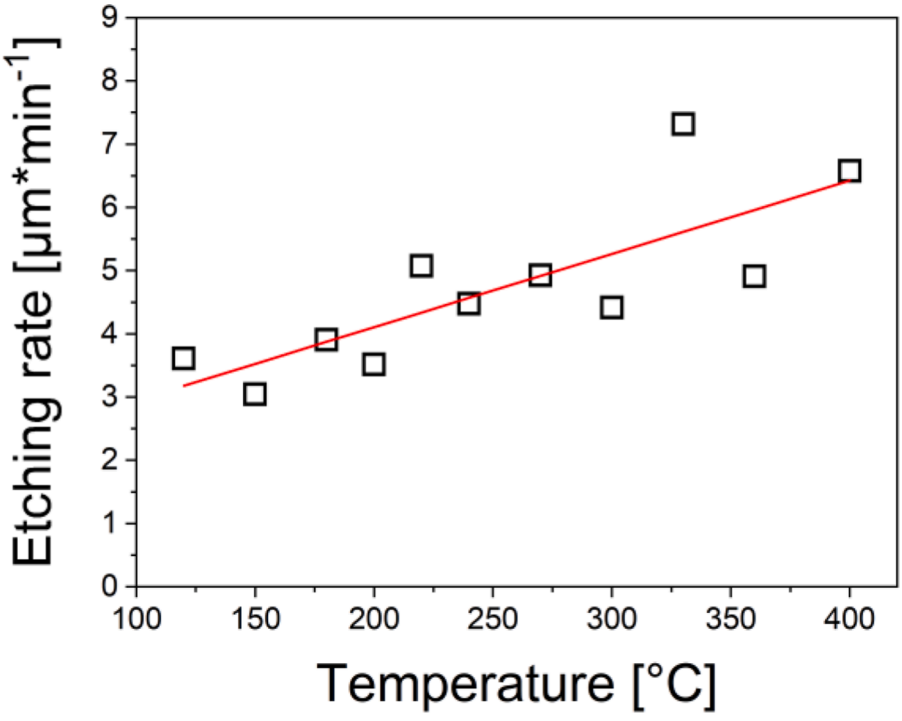

Fig. 4. Etching rate in dependence on substrate temperature for otherwise fixed etching conditions. Parameter: t_E= 3 min; E_P = 920 μJ, d_{PS} = 140 μm, p_{tot}= 800 mbar, O_2 = 17 vol.-%.

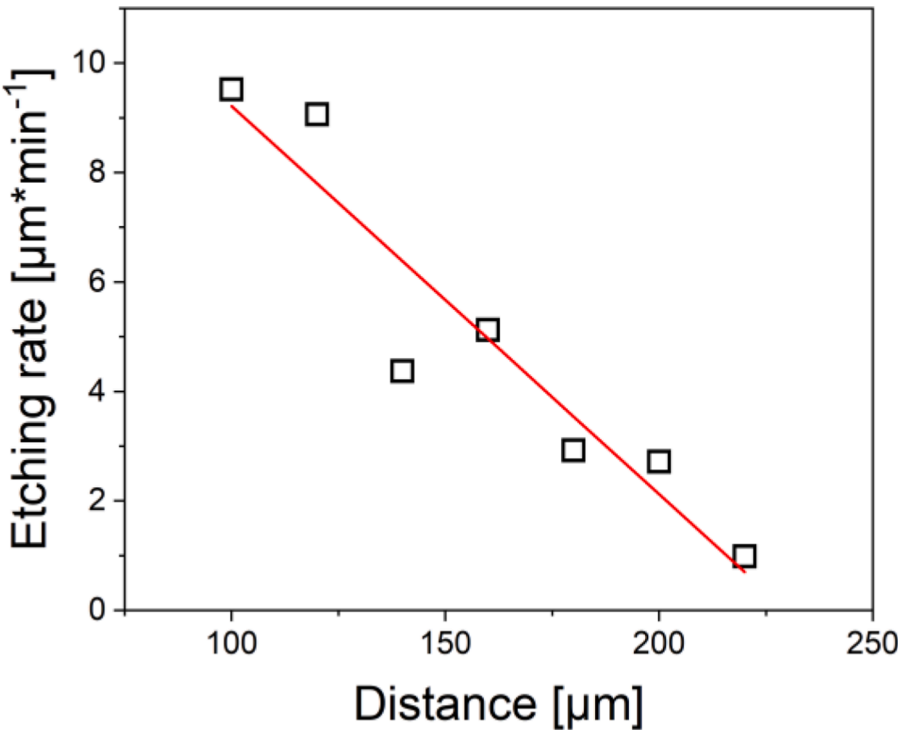

Fig. 5. Relation between etching rate and plasma-surface distance including a linear fit that suggest a threshold distance of 230 µm. Parameter: t_E= 3 min, E_P = 900 µJ, T_S = 230 °C, p_{tot}= 800 mbar, O_2= 17 vol.-%.

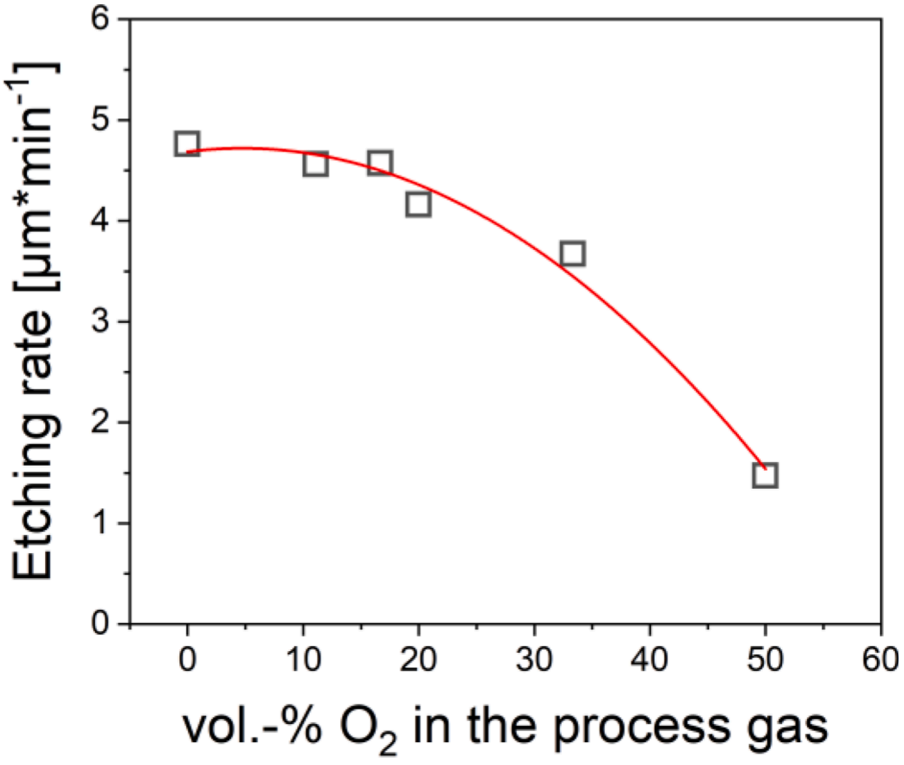

Fig. 6. Etching rate in dependence on oxygen concentration for otherwise constant etching conditions. Parameter: t_E= 3 min, E_P = 1070 µJ, T_S = 230 °C, d_{FS} = 140 µm, p_{tot} = 800 mbar, O_2 = 17 vol.-%.

Significant changes of the surface morphology of <100>Si occur during the etching process as shown in Fig. 10. The pristine substrates surface is smooth with a roughness of R_q < 1 nm. Structures at different scales appear. The size of the LIP determines the overall etching groove. However, much smaller etching pits with micrometre size appear and get steeper with ongoing silicon etching.

These patterns have always a maximal depth near the centre that looks like a point. Surprisingly, the etching pits show the tendency of

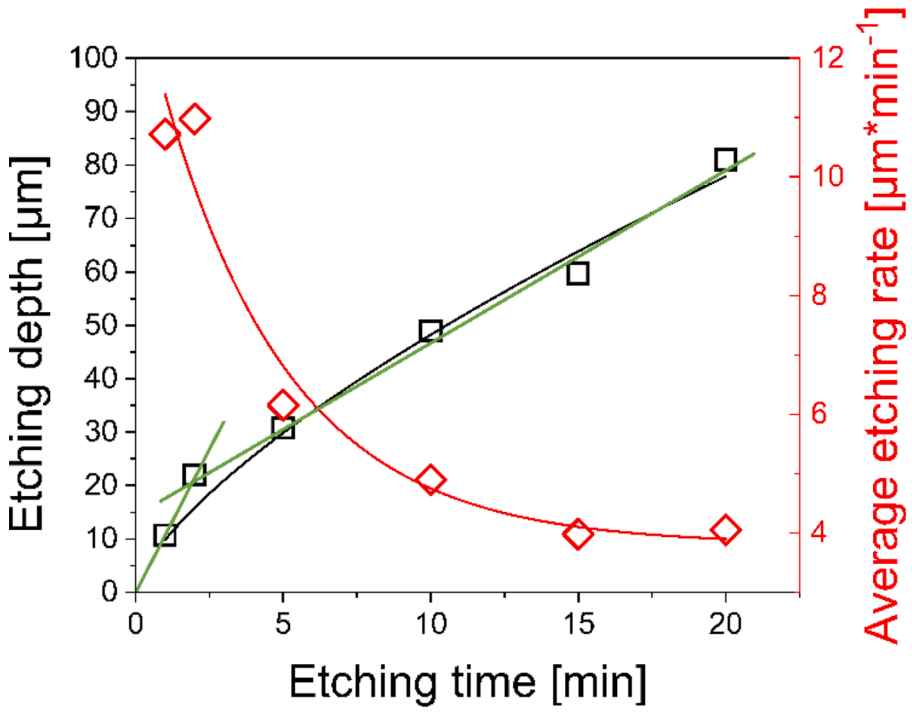

Fig. 7. Influence of etching duration on the etching depth and the average etching rate at fixed etching conditions. Parameter: E_P = 880 µJ, T_S = 330 °C, d_{PS} = 140 µm, p_{tot} = 800 mbar, O_2 = 17 vol.-%.

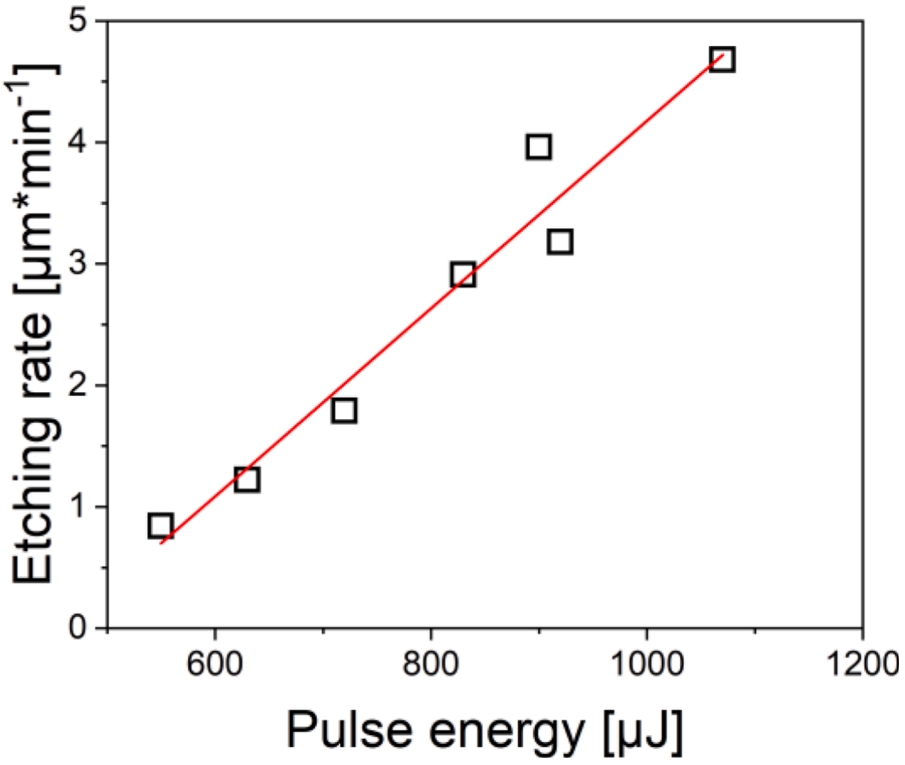

Fig. 8. Dependence of the etching rate on the pulse energy. A linear relation with a threshold of 460 µJ can be seen. Parameter: t_E= 5 min, T_S = 230 °C, d_{FS} = 140 µm, p_{tot} = 800 mbar, O_2 = 17 vol.-%.

forming inverse pyramids at a total etching depth of approximately 8 µm. While the sizes of the pyramids vary strongly, the incline of the pyramid walls is in the range of 20–30°. With further increasing etching time and therefore also etching depth, the pyramids disappear and the pits are shell-shaped with an enlarged lateral size. Neighbouring pits coalescence, forming bigger pits. At this stage the surface of each is smooth, but still curved. This development of the surface morphology with the etching time can be seen in Fig. 10. For <110> and <111>-orientations a similar formation of etching pits was observed, but there were no signs of crystallographic etching.

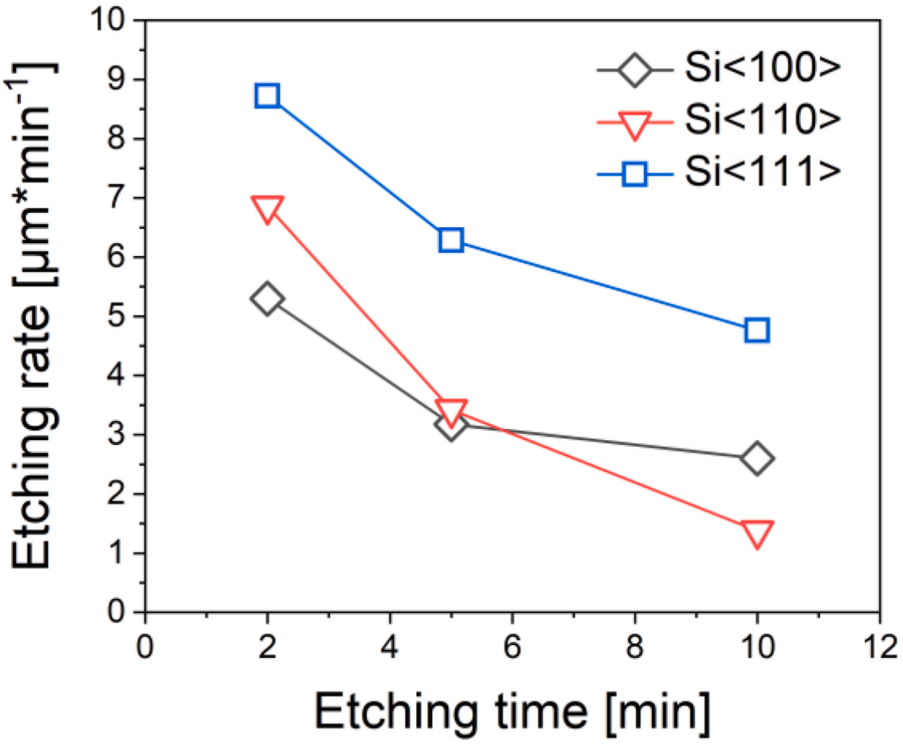

Fig. 9. Etching rates of silicon for different crystal orientations in dependence on the etching time. Parameter: E_P = 920 µJ, T_S = 230 °C, d_{PS} = 140 µm, p_{tot} = 800 mbar, O_2 = 17 vol.-%.

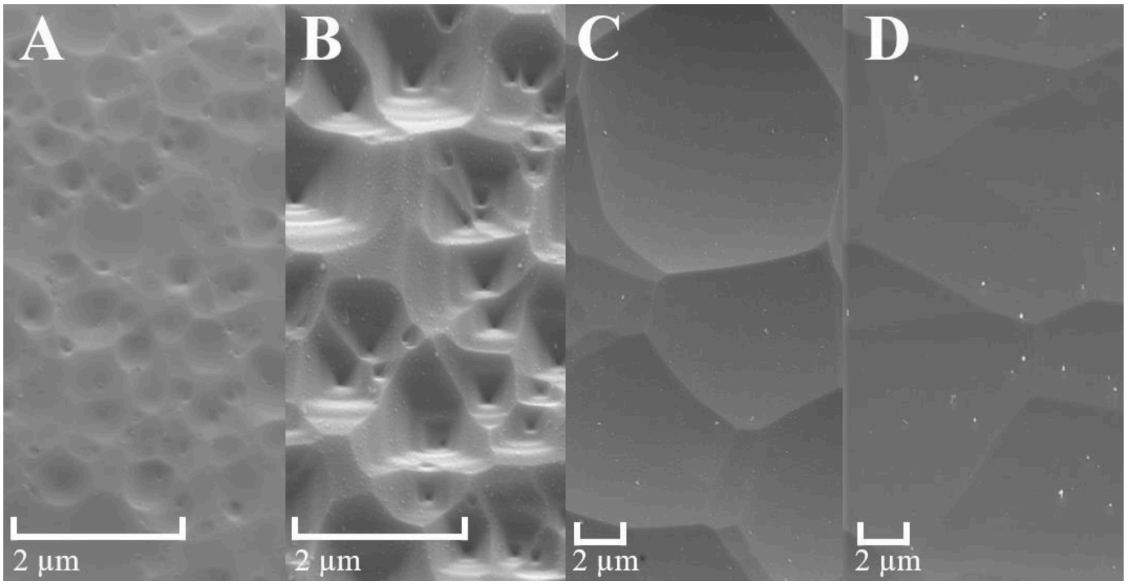

Fig. 10. SEM-images of etching groove surfaces of <100>Si at different etching times (etching depths; roughness). A: 0.5 min (5 µm; 8 nm rms); B:1 min (10 µm; 170 nm rms); C: 5 min (30 µm; 45 nm rms); D: 20 min (80 µm; 20 nm rms); (Image C and D have been taken with a different magnification).

Due to the expected chemical nature of the LIP etching process, the temperature in relation to the surface morphology needs to be evaluated too. Fig. 11 shows the surface morphology of LIP etched silicon with increasing substrate temperatures. At a temperature of 160 °C, the surface is riddled with pits of different sizes and various shapes, but most of them have a diameter of less than 500 nm. The surface becomes smoother with increasing temperature. A rather rough surface with local etching pits with a more uniform size distribution of 1 µm on average and rather steep side walls occurs at 200 °C substrate temperature. Samples that are etched in a temperature range of 200 °C to <400 °C, are less smooth compared to 180–200 °C. The size of the pits increases with temperature. At a substrate temperature of 400 °C a smooth surface with almost no pits and a micro roughness of less than 5 nm rms (AFM) was found.

Experiments at a substrate temperature of 250 °C have shown, that less rough surfaces can be also attained with other etching parameters, as illustrated in Fig. 12. Reducing the pulse energy results in smoother surfaces at the same etching depth. However, the etching rate reduces with lower pulse energies, which extends the time needed to remove the same amount of material. Increasing the plasma-surface distance, a

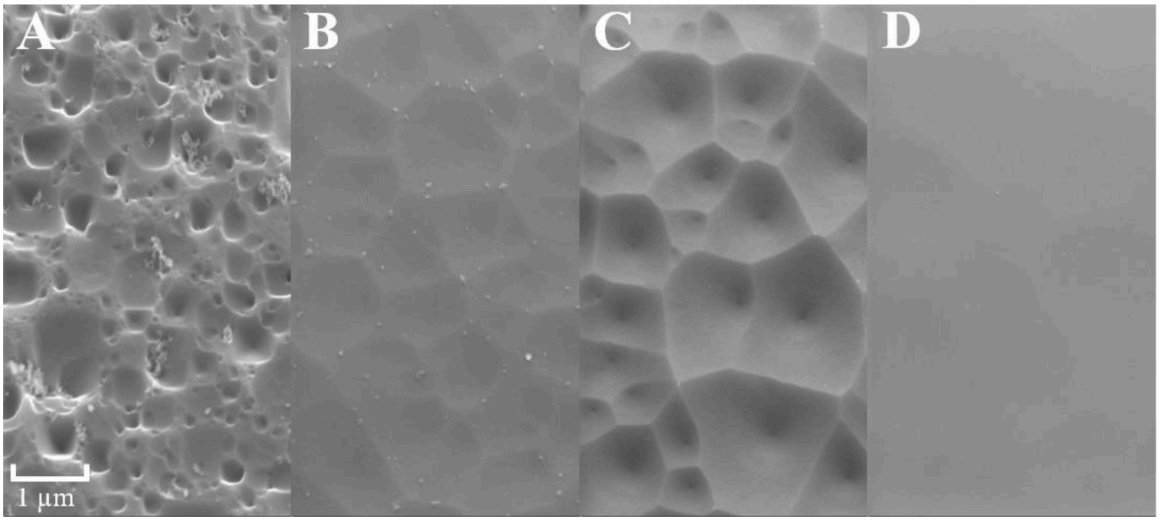

Fig. 11. SEM-images of etched <100>-silicon with different temperatures. A) 160 °C (18 nm rms); B) 200 °C (10 nm rms); C) 240 °C (80 nm rms); D) 400 °C (4 nm rms).

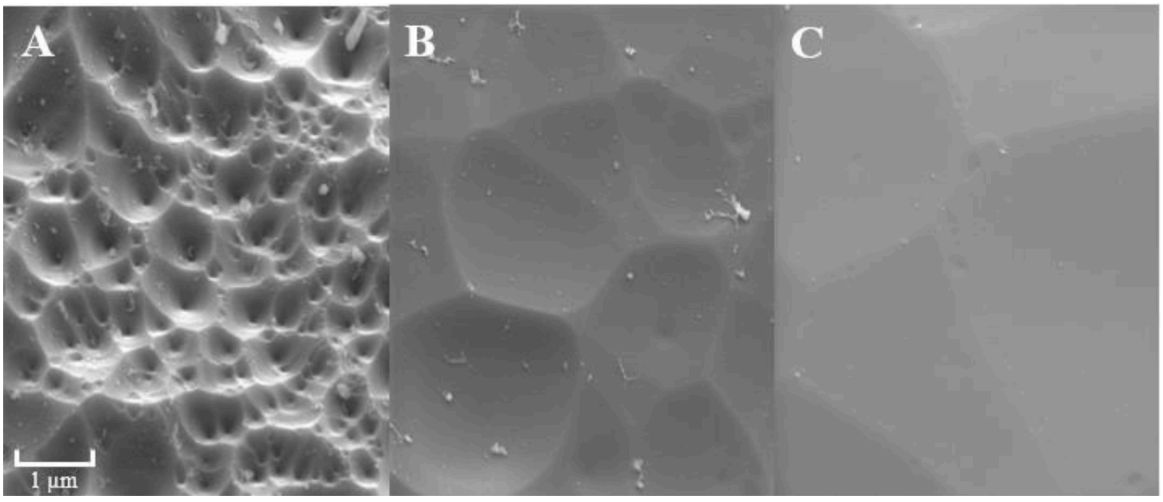

Fig. 12. SEM-images of etched <100>silicon. A) d_{PS}= 140 µm E_P= 900 µJ, t_E= 3 min with a maximal depth of 20 µm; B) d_{PS}= 200 µm, E_P= 900 µJ, t_E= 3 min with a maximal depth of 8 µm; C) d_{PS}= 140 µm, E_P= 720 µJ, t_E= 30 min with a maximal etching depth of 20 µm.

reduced roughness for the same etching time has been found. However, both the etching depth as well as the etching rate needs to be considered for evaluation of particular etching conditions.

4. Discussion

During the etching of silicon with a laser-induced micro plasma many different physical and chemical processes occur simultaneously, which can lead to a complex relation of process parameters and etching results. Considering typical dry etching processes, the laser-induced plasma etching mechanism can be divided into five basic stages. (I) excitation of the plasma in the gas mixture by optical break through, (II) formation of reactive species due to decomposition of gas components, (III) transport of reactive species to the surface, (IV) interaction and reaction of different plasma specimens with the substrate material forming reaction products, and (V) desorption of volatile reaction products resulting in material removal [1,16].

Despite that all processes can be rate limiting usually one step of the mechanism is the rate limiting process that is in some cases linked to a process parameter. However, the rate limiting step is not necessarily fixed over the whole experimental parameter range but can alter in dependence on the actual experimental parameter set chosen.

Hence, the main mechanisms to keep in mind for discussion are the chemical reaction, that is substantial governed by the temperature and the reactive species concentration at the samples surface, the concentration driven diffusion of species and reaction products, the feed of fresh gas and the exhaust of degraded gas and the formation of reactive species in the LIP. In addition to these macroscopic considerations, microscopic processes can influence the etching, that are related, e.g., to material defects and material/surface impurities.

Silicon etching with CF_4 species, that are generated in the plasma, is based on the chemical reaction of silicon with fluorine radicals. Therefore, one limiting factor in terms of etching rate is the quantity of reactive species at the silicon sample surface. It can be assumed, that an increase of the laser pulse energy and therefore stronger excitation of the plasma causes a higher amount of reactive species in the LIP, that can result in higher etching rates as observed in the experiments (see Fig. 8). Such a linear increase of the etching rate with the power of the plasma is also observed in low pressure plasma etching of silicon [22–24]. As the laser power can be correlated with the power for plasma excitation these experimental findings are in line with former results.

Higher plasma substrate distances influence the transport path of

reactive species to the silicone surface, causing an etching rate decrease with higher distances. The diffusion of fluorine radicals needs time and should have an R^2 dependence, as the laser-induced plasma can be considered as a laser-driven point source of radicals. In terms of the radical flow, diffusion, or density, the experimental determined plasma distance dependence (see Fig. 5) cannot be fully explained by such transport processes. The transport of plasma-generated species is different to traditional plasma etching processes such as RIE and PE, due to the nearly atmospheric pressures. The mean free path length for these experiments is approximately 10^3 times smaller than the plasma surface distance, resulting in a high number of collisions and interactions of the plasma species during the diffusion. Those interactions can lead to the consumption of reactive species by side reaction or deactivation of radicals. The number of collisions increases with increasing distance and therefore the amount of reactive fluorine radicals reaching the surface decreases, resulting in lower etching rates. This must be discussed as a dynamic process as the plasma is pumped by a very short laser pulse and has an assumed live time of 10 μs. This dynamic of the pulsed plasma and the breakdown-induced shockwave should influence the transport mechanisms too and need to be subject of further investigations. These results can also be useful to explain the shape of the etching groove and its time dependence, which are not fully understood yet.

For all experiments the influence of the growing depth of the etching groove should be discussed. Since there is a decreasing etching rate for higher plasma surface distances the results can be strongly distorted, especially for deep etching grooves (80 μm etching groove with a distance of 220 μm to the plasma instead of 140 μm). Comparing the results of the varied plasma-surface distances to the results of the varied process times lead to the assumption, that the influence of the distance is a lot higher for flat surfaces than for the etching grooves. The etching rate is nearly constant after 5 min of etching, while the distance to the plasma still increases. Therefore, the steepening etching groove may lead to an enhanced concentration of fluorine radicals in the center of the footprint.

Various effects arise as the temperature increases, that result in different etching rates and surface morphologies. The sticking probability of CF_x decreases at higher temperatures and the desorption rate increases. This reduces, or even prevents the deposition of fluorine polymers and thereby the masking of the silicon by a thin film during etching [25]. Other important parameters significantly influenced by the temperature are the composition of the resulting reaction products and the layer thickness of Si_xF_y -compounds on the surface. With increasing temperature, the amount of SiF_2 as a volatile product gets higher, while the amount of SiF_4 decreases. So, with the same number of F*, more material can be removed with increasing temperature [26].

Since most of the products of the Si-F reaction do not instantly volatilize but likely build a layer of Si_xF_y on the substrate surface, diffusion processes of F* through this layer have an impairing influence on the etching rate. Studies show [27,28], that the silicon-fluorine-layer thickness reduces with an increasing temperature, resulting in higher etching rates. Therefore, with increasing temperature a potentially formed fluorocarbon or Si_xF_y layer is reduced in thickness and the reaction rate should be increased, according to Arrhenius equation: both result in a higher etching rate. For further studies, the dynamics of the pulsed plasma should also be considered in terms of temperature, since temporary temperature differences can be expected due to the proximity of the plasma to the silicon surface.

The next parameter to be considered is the gas composition. An addition of oxygen to CF_4 can have some advantages for reactive plasma etching. The first one to be found in studies is an increase in fluorine radical density in RIE plasmas due to the prevention of recombination with CF_x compounds by a reaction with the oxygen to COF_2. A side effect of this reaction is, that less CF_x can migrate to the silicon surface that results in less build-up of a CF_x-polymer film on the surface. These processes should increase the etching rate as observed for RIE processes in [29], but this cannot be confirmed for LIP silicon etching, because of the constant etching rates for 0–17 vol.-% of oxygen. Reasons can be the higher pressure, the high molecular collisions and the low kinetic energy of the species impinging the surface. An effect that can be confirmed is the reducing etching rate for much higher amounts of oxygen. This process could be a result of a $Si_xO_yF_z$-layer at the surface, because increasing oxygen radicals cause different reaction in the gas phase as well as at the surface [29,30]. It is also possible that an increasing formation of silicon oxide with higher oxygen radical concentrations leads to a reduced etching rate, because SiO_2 gets removed slower than Si, as it can be seen by comparing the results of Ehrhardt et al. with the results of this paper [16].

The dramatically change of the etching rate with time cannot be explained by reduced radical densities or additional laser-induced heating. Therefore, the formation of transient layers (CF_x, Si_xF_y, etc.) on the surface can be dominating processes, causing the process time dependence of the etching rate. During the process the layer thickness increases, enhancing the resistance for fluorine radicals diffusing to the surface. In this process stage the etching rate drops until a balance of layer building and layer removing processes is achieved. Another factor, that should be considered, is the etching enhancing effect of mechanical defects and chemical impurities near the silicon surface. Such defects cause usually an enhanced chemical reaction due to the already weakened surface [31]. Since most of these defects originate from the silicon wafer separation process and subsequent incidents, their frequency gradually decreases with increasing distance from the surface.

As the defects are localized and better etchable the formation of etching pits, as experimentally found, are not surprising and support strongly the chemical dry etching mechanism.

While etching, the surface morphology changes significantly and may influence the interaction with the LIP in relation to the surface area as well as the inclination to reactive species.

The observable roughening of the surface at the beginning of the etching process may be due to the different sticking coefficients of plasma species or an inhomogeneous silicon surface. In this relation defects are the preferential candidate for such initial roughening [31]. This nano roughness may develop by topography induced effects. As described in [32] the sticking probability for CF_x is higher than for F*. The fluorine radicals reflect on the surface more often and so shadowing effects of CF_x-compounds need to be considered. The difference in the sticking coefficients leads to a concentration difference between hills and valleys of a topographical surface:

$$\left(\frac{n_{F^*}}{n_{CF_x}}\right)_{valley} > \left(\frac{n_{F^*}}{n_{CF_x}}\right)_{hill} \quad (1)$$

resulting in a faster etching rate of the valleys and therefore the formation of pits. While the pits become steeper, a point of maximal depth forms inside of the etching pits (Fig. 11c), that may be the starting point for the formation of inverse pyramids due to crystallographic etching. This could be an effect of the different etching rates on differently oriented crystal planes, with <111> being the fastest. For that reason, <100> and <110> planes may be removed slower and form these stepwise pyramidal structures.

The smoothening effects for higher etching times might relate to the coalescence of inverse pyramids reducing <111> planes density. Further, longer etching times – meaning higher etching depths – results in the reduction of the defect density and therefore in the reduction in the inverse pyramid forming probability. A supporting effect could be the formation of the Si_xF_y- or $Si_xO_yF_z$-layer, that limits the etching rate to the speed of diffusion of F* through the layer and equalizes the concentration difference, resulting in a faster etching of roughness peaks.

The temperature has a significant impact on the surface morphology. As described in previous sections, the effects of an increased surface temperature are complex and influence each other. Since there is not yet sufficient knowledge about the occurring processes and their interaction, we can only speculate at this point. One smoothing effect at

increased temperatures may be the higher surface mobility of the adsorbed CF_x, resulting in reduction of shadowing effects. For temperatures above 200 °C, processes that amplify the roughening of the surface seem to become more dominant. For the range between 200 and 400 °C, the surface morphology looks similar, so there appears to be a balance in temperature dependence between roughening and smoothing phenomenon. Etching grooves at a substrate temperature of 400 °C probably stay smooth, because it is too high for a deposition of CF_x or the resulting polymer, so no masking effects can occur. In summary, the temperature provides the energy for the chemical reaction for etching. Temperature changes probably result in the change of the balance between all involved near surface processes, that can result in changed rate differences between the crystallographic orientations as well as the etch rate of contaminated or defect rich silicon.

The complex interaction of all processes involved in LIP etching of silicon needs further investigations in the gas phase, the silicon surface and the laser-induced plasma ignition, considering in general that each has a particular dynamic.

5. Conclusions

Dry etching of silicon by a laser-induced plasma in a CF_4/O_2 mixture has been demonstrated and studied. Different surface morphologies and etching rates can be observed as a consequence of the utilized process parameters. With a pulse energy of ≈1000 μJ and a plasma-surface distance <150 μm etching rates up to 12 μm x min^{-1} can be achieved. The etching rate can be adjusted easiest by the variation of pulse energy and plasma-surface distance; both show a linear relation to the etching rate. The surface morphology was mainly influenced by the surface temperature, where the smoothest surfaces with a roughness < 5 nm rms have been found at 400 °C. The etching rate decreases during the etching process, probably because of the formation of an inhibiting CF_x, Si_xF_y- or $Si_xO_yF_z$-layer.

The presented etching method provides an approach for precise machining of silicon surfaces with good surface qualities near atmospheric pressure and sufficiently high material removal rates for ultra-precise surface machining. The investigations show that the process is chemically dominated without any signs of mechanical or thermal damages, as it can be observed for laser processing. Due to the small footprint and low removal rates per laser pulse it can be a powerful tool for the manufacturing or correction of MEMS and free form optics.

Acknowledgments

The authors wish to acknowledge the help of Ms. I. Mauersberger with the SEM and AFM measurements. This work was funded by the Deutsche Forschungsgemeinschaft (DFG, German Research Foundation) - No. 392226212.

References

[1] P. Schaaf, Laser Processing of Materials: Fundamentals, Applications and Developments, 139, Springer Science & Business Media, 2010.
[2] A. Fridman, Plasma Chemistry, Cambridge university press, 2008.
[3] M. Köhler, Ätzverfahren für Die Mikrotechnik, Wiley Online Library, 1998.
[4] V.M. Donnelly, A. Kornblit, Plasma etching: yesterday, today, and tomorrow, J. Vacuum Sci. Technol. A 31 (5) (2013), 050825.
[5] T. Arnold, et al., Ultra-precision surface finishing by ion beam and plasma jet techniques-status and outlook, Nucl. Instrum. Methods Phys. Res. Sect. a-Acceler. Spectrom. Detect. Associat. Equip. 616 (2–3) (2010) 147–156.
[6] M. Weiser, Ion beam figuring for lithography optics, Nucl. Instrum. Methods Phys. Res. Sect. B 267 (8) (2009) 1390–1393.
[7] A. Schutze, et al., The atmospheric-pressure plasma jet: a review and comparison to other plasma sources, IEEE Trans. Plasma Sci. 26 (6) (1998) 1685–1694.
[8] F. Kazemi, G. Boehm, T. Arnold, An investigation on effectiveness of temperature treatment for fluorine-based reactive plasma jet machining of N-BK7®, Plasma Processes Polym. 17 (8) (2020), 2000016.
[9] T. Ichiki, R. Taura, Y. Horiike, Localized and ultrahigh-rate etching of silicon wafers using atmospheric-pressure microplasma jets, J. Appl. Phys. 95 (1) (2004) 35–39.
[10] H. Paetzelt, G. Böhm, T. Arnold, Etching of silicon surfaces using atmospheric plasma jets, Plasma Sources Sci. Technol. 24 (2) (2015), 025002.
[11] T. Arnold, G. Boehm, A. Schindler, Ultrahigh-rate plasma jet chemical etching of silicon, J. Vacuum Sci. Technol. A 19 (5) (2001) 2586–2589.
[12] K. Zimmer, R. Böhme, Laser-induced backside wet etching of transparent materials with organic and metallic absorbers, Laser Chem. 2008 (2008).
[13] M. Ehrhardt, et al., Laser-induced backside wet etching of fluoride and sapphire using picosecond laser pulses, Appl. Phys. A 101 (2) (2010) 399–404.
[14] S. Elhadj, et al., Laser-induced gas plasma etching of fused silica under ambient conditions. Laser-Induced Damage in Optical Materials: 2012. 2012. International Society For Optics and Photonics, 2012.
[15] S. Elhadj, et al., Laser-based dynamic evaporation and surface shaping of fused silica with assist gases: a path to rimless laser machining, Appl. Phys. B 113 (3) (2013) 307–315.
[16] M. Ehrhardt, et al., Laser-induced reactive microplasma for etching of fused silica, Appl. Phys. A 126 (11) (2020) 1–9.
[17] A.W. Miziolek, V. Palleschi, I. Schechter, Laser Induced Breakdown Spectroscopy, Cambridge university press, 2006.
[18] J.P. Singh, S.N. Thakur, Laser-induced Breakdown Spectroscopy, Elsevier, 2020.
[19] D.W. Hess, K.A. Reinhard, Plasma stripping, cleaning, and surface conditioning, Handb. Silicon Wafer Clean. Technol. 2 (2008) 355.
[20] H. Ibach, H. Lüth, Festkörperphysik: Einführung in Die Grundlagen, springer-verlag, 2009.
[21] H. Seidel, et al., Anisotropic etching of crystalline silicon in alkaline solutions: I. Orientation dependence and behavior of passivation layers, J. Electrochem. Soc. 137 (11) (1990) 3612.
[22] C. Cardinaud, Fluorine-based plasmas: main features and application in micro-and nanotechnology and in surface treatment, C. R. Chim. 21 (8) (2018) 723–739.
[23] C. Mogab, The loading effect in plasma etching, J. Electrochem. Soc. 124 (8) (1977) 1262.
[24] Y.J. Lii, et al., Plasma etching of silicon in SF 6: experimental and reactor modeling studies, J. Electrochem. Soc. 137 (11) (1990) 3633.
[25] D.M. Mattox, Handbook of Physical Vapor Deposition (PVD) Processing, William Andrew, 2010.
[26] B.J. Garrison, W.A. Goddard III, Reaction mechanism for fluorine etching of silicon, Phys. Rev. B 36 (18) (1987) 9805.
[27] K. Ninomiya, et al., Reaction of atomic fluorine with silicon, J. Appl. Phys. 58 (3) (1985) 1177–1182.
[28] P. Verdonck, et al., Importance of fluorine surface diffusion for plasma etching of silicon, J. Vacuum Sci.& Technol. B 20 (3) (2002) 791–796.
[29] C. Mogab, A. Adams, D. Flamm, Plasma etching of Si and SiO2—the effect of oxygen additions to CF4 plasmas, J. Appl. Phys. 49 (7) (1978) 3796–3803.
[30] G. Oehrlein, et al., Study of plasma-surface interactions: chemical dry etching and high-density plasma etching, Plasma Sources Sci. Technol. 5 (2) (1996) 193.
[31] R. Petri, et al., Silicon roughness induced by plasma etching, J. Appl. Phys. 75 (11) (1994) 7498–7506.
[32] E. Gogolides, et al., Controlling roughness: from etching to nanotexturing and plasma-directed organization on organic and inorganic materials, J. Phys. D 44 (17) (2011), 174021.